HDM-2 inhibition suppresses expression of ribonucleotide reductase subunit M2, and synergistically enhances gemcitabine-induced cytotoxicity in mantle cell lymphoma

Richard J. Jones,[1] Veerabhadran Baladandayuthapani,[2] Sattva Neelapu,[1] Luis E. Fayad,[1] Jorge E. Romaguera,[1] Michael Wang,[1] Rakesh Sharma,[1] Dajun Yang,[3] and Robert Z. Orlowski[1,4]

[1]Department of Lymphoma and Myeloma, The University of Texas M. D. Anderson Cancer Center, Houston, TX; [2]Department of Biostatistics, The University of Texas M. D. Anderson Cancer Center, Houston, TX; [3]Ascenta Therapeutics Inc, Malvern, PA; and [4]Department of Experimental Therapeutics, The University of Texas M. D. Anderson Cancer Center, Houston, TX

Mantle cell lymphoma (MCL) usually responds well to initial therapy but is prone to relapses with chemoresistant disease, indicating the need for novel therapeutic approaches. Inhibition of the p53 E3 ligase human homolog of the murine double minute protein-2 (HDM-2) with MI-63 has been validated as one such strategy in wild-type (wt) p53 models, and our genomic and proteomic analyses demonstrated that MI-63 suppressed the expression of the ribonucleotide reductase (RNR) subunit M2 (RRM2). This effect occurred in association with induction of p21 and cell-cycle arrest at G_1/S and prompted us to examine combinations with the RNR inhibitor 2′,2′-difluoro-2′-deoxycytidine (gemcitabine). The regimen of MI-63–gemcitabine induced enhanced, synergistic antiproliferative, and proapoptotic effects in *wtp53* MCL cell lines. Addition of exogenous dNTPs reversed this effect, whereas shRNA-mediated inhibition of RRM2 was sufficient to induce synergy with gemcitabine. Combination therapy of MCL murine xenografts with gemcitabine and MI-219, the in vivo analog of MI-63, resulted in enhanced antitumor activity. Finally, synergy was seen with MI-63–gemcitabine in primary patient samples that were found to express high levels of RRM2 compared with MCL cell lines. These findings provide a framework for translation of the rational combination of an HDM-2 and RNR inhibitor to the clinic for patients with relapsed *wtp53* MCL. (*Blood*. 2011; 118(15):4140-4149)

Introduction

Mantle cell lymphoma (MCL) is a B-cell lymphoma that accounts for 6% to 8% of lymphoid malignancies and typically harbors the t(11;14) translocation, resulting in aberrant cyclin D1 expression and cell-cycle dysregulation.[1] MCL patients present with a spectrum of disease types ranging from slow, indolent growing malignancies to more aggressive variants, such as the blastoid phenotype. It is characterized clinically by good initial responses to induction chemotherapy, but later it almost invariably relapses with a more aggressive course,[1] making it an attractive model for novel drug development.[2,3] One such novel agent is the proteasome inhibitor bortezomib that was shown to be active against MCL in a phase 1 trial[4] and then approved for treatment of relapsed disease after multicenter studies fully demonstrated its activity.[5-7] Other drugs that have shown promise against MCL include novel agents such as the mammalian target of rapamycin inhibitors temsirolimus[8] and everolimus,[9] the immunomodulatory drug lenalidomide,[10,11] and more traditional cytotoxics such as (2′,2′-difluoro-2′-deoxycytidine (gemcitabine, dFdC).[12,13]

dFdC is an effective, broad-spectrum anticancer agent with activity in many malignancies, including as a single agent and in combination for non-Hodgkin lymphoma.[14] It is transported into the cell mainly through the human equilibrative nucleoside transporter (hENT)-1,[15] where it is metabolized by deoxycytidine kinase (dCK) into its 2 active forms, dFdC-diphosphate and dFdC-triphosphate (dFdCTP).[16] The cytotoxic effects of dFdC are because of the ability of dFdC-diphosphate to inhibit the function of ribonucleotide reductase (RNR) and of dFdCTP to compete with dCTP for incorporation into DNA.[17-19] dFdC-phosphate is identified by RNR as a substrate, metabolized within the active site, and then generates mutated products that inactivate the R1 subunit (RRM1) and induce the loss of the tyrosyl radical essential for action of the R2 subunit (RRM2). This produces a global decrease in the level of available cellular dNTPs for DNA replication. In addition, the dFdCTP moiety competes with cellular dCTP for insertion into DNA, after which DNA chain termination occurs and replication ceases.[16] dFdC is highly effective in part because of this dual action, particularly because RNR overexpression is correlated with enhanced invasive potential, malignant transformation, and metastasis,[20] and because overexpression by malignant cells conveys a selectivity that helps to reduce toxicity to normal cells.

Another attractive target for MCL therapy may be the p53 pathway, because DNA damage responses are altered in up to 75% of cases, in part through mutations of ataxia telangiectasia mutated[21] or p53.[21,22] Overexpression of the human homolog of the murine double minute protein-2 (HDM-2), which is seen in 22% or more of MCL cases, has also been associated with a more aggressive course and decreased survival.[23-28] This may be due in part to its ability to decrease p53 levels through its activity as the major E3 ubiquitin

Submitted March 3, 2011; accepted August 8, 2011. Prepublished online as *Blood* First Edition paper, August 15, 2011; DOI 10.1182/blood-2011-03-340323.

The online version of the article contains a data supplement.

The publication costs of this article were defrayed in part by page charge payment. Therefore, and solely to indicate this fact, this article is hereby marked "advertisement" in accordance with 18 USC section 1734.

ligase responsible for p53 ubiquitination before its proteasome-mediated degradation.[29] Consistent with the possibility that nongenotoxic stabilization of p53 may be a valid approach to therapy of MCL, we and others have demonstrated previously the activity of HDM-2 inhibitors such as the Nutlins, and MI-63 and MI-219 against wild-type (wt) p53 MCL models both in vitro and in vivo.[30-33] In this current work, we report the development of a mechanism-based combination regimen, which started with the observation that MI-63 decreased the expression levels of RRM2. By combining an HDM-2 inhibitor with dFdC, we were able to demonstrate that this regimen showed enhanced activity against MCL cell lines and xenografts compared with either agent alone. This approach may prove fruitful for the treatment of patients with relapsed, *wtp53* MCL, and is ready for translation to the clinic.

Methods

Reagents

The HDM-2 inhibitors MI-63 and MI-219 were provided by Ascenta Therapeutics. Nutlin-3, dFdC for in vitro work, doxorubicin, and deoxyribonucleotides (dNTPs) were purchased from Sigma-Aldrich, whereas dFdC for in vivo work was from the M. D. Anderson Cancer Center Clinical Pharmacy.

Cell culture and patient samples

JVM-2, Granta-519, REC-1, and JeKo-1 MCL cell lines were purchased from the German Collection of Microorganisms and Cell Cultures and validated through The M. D. Anderson Cancer Center Characterized Cell Line Core Facility. Cells were grown in RPMI 1640 (Invitrogen) supplemented with 10% FBS, 100 U/mL penicillin, and 100 μg/mL streptomycin (Sigma-Aldrich). Primary patient samples were obtained from the M. D. Anderson Department of Lymphoma and Myeloma Satellite Lymphoma Tissue Bank. Informed consent was obtained from each patient in compliance with the Declaration of Helsinki according to an M. D. Anderson Cancer Center Institutional Review Board-approved protocol, and samples were purified as described previously.[30]

Semiquantitative and real-time PCR

Total RNA was isolated using an RNeasy Plus kit (QIAGEN), and cDNA was synthesized using SuperScript II (Invitrogen). PCR was performed for 30 cycles annealing at 54.4°C for RRM2 (GenBank accession NM_001165931) using sense primer 5′-GAAGGCAGAGGCTTCCTTTT-3′ and antisense primer 5′-AGAAACAGCGGGCTTCTGTA-3′ and for the p53-inducible R2 subunit (R2p53, or p53-inducible RNR subunit M2B [RRM2B]; GenBank accession NM_015713) using sense primer 5′-GGGGATTCTGTGGTCAGATG-3′ and antisense primer 5′-GGCCAGCTTTTTCCAATCTT-3′. Primers and conditions for β_2-microglobulin (β_2M), which was used as a control, were as described previously.[34] Real-time PCR for RRM1, RRM2, RRM2B, dCK, and hENT-1 was performed on a StepOne PCR analyzer (Applied Biosystems) using inventoried real-time TaqMan-FAM and GAPDH-VIC probes. Relative transcript expression (RQ) was determined using JVM-2 cells as a calibrator using the ΔΔCT method according to the manufacturer's instructions (Applied Biosystems).

p53 sequencing

Genomic DNA was extracted from MCL patient samples, and all exons, introns, and regulatory regions of p53 were sequenced by the M. D. Anderson DNA Analysis Core Facility. Exons were amplified using custom PCR primers, and Sanger sequencing was performed on a 3730xl DNA analyzer using BigDye Terminator v3 chemistry (Applied Biosystems). Mutations analysis was performed using SeqScape Version 2.5 software (Applied Biosystems).

Gene expression profiling

RNA was extracted from MI-63– or vehicle-treated cells using TRIzol (Invitrogen) in triplicate, and RNA was submitted to Genome Explorations for gene expression profiling analysis using the Affymetrix Human Genome U133 Plus 2.0 array platform.

Immunoblotting

Protein expression was measured by immunoblot analysis performed as described previously.[34] Antibodies to RRM1, RRM2, RRM2B, and p53 were purchased from Santa Cruz Biotechnology, the anti-poly(ADP-ribose) polymerase (PARP) antibody was from Cell Signaling Technology, anti-p21 and anti–HDM-2 antibodies were purchased from EMD4Biosciences, and the anti–β-actin antibody was from Sigma-Aldrich.

Cell-cycle and cell-death analysis

Cells were treated with drug for 24 hours and then fixed in 70% ethanol and stained with propidium iodide (Sigma-Aldrich). Cell-cycle data were analyzed on a CANTO II flow cytometer (BD Biosciences) using FlowJo Version 7.6.1 (TreeStar). Cell death also was measured using annexin-V Pacific Blue and TO-PRO-3 (Invitrogen) on a CANTO II flow cytometer using FlowJo Version 7.6.1.

Cell-proliferation assay

The WST-1 reagent (Roche Diagnostics) was used to determine the effects of chemotherapy agents on cell proliferation and to calculate their relative IC_{50} values, as published previously.[35]

Lentiviral shRNA knockdown of RRM2

Lentiviral shRNA particles (Santa Cruz Biotechnology) containing either a scrambled sequence shRNA or shRNAs targeting RRM2 were transduced overnight at a multiplicity of infection of 2 into REC-1 MCL cells. These cells were then drug selected with 2 μg/mL puromycin (Sigma-Aldrich) to generate stable cell lines.

Drug synergy assays

To evaluate for the presence of synergistic interactions, the methods of Chou and Talalay were used as described previously.[36,37] In brief, MI-63 or dFdC was added to cells, and the IC_{50} value of each drug individually was determined using the WST-1 assay. A range of serial dilutions was made across the IC_{50} dose range, with the IC_{50} set as 1×, and dilutions were made relative to this value. The agents were then added simultaneously to the cells or in a sequence-specific order for 3 days, and WST-1 assays were performed. Data were then analyzed using CalcuSyn Version 2 software (Biosoft), and combination indices (CIs) were calculated.

In vivo xenograft model

Experiments were performed in accordance with procedures and protocols approved by the M. D. Anderson Cancer Center Animal Care and Use Committee. Six- to 8-week-old male CB-17 severe combined immunodeficiency mice (Harlan) were inoculated in the right flank subcutaneously with 5×10^6 Granta-519 cells. Tumor burden was monitored by measuring the length and width of visible masses using calipers 3 times per week, and tumor volumes were calculated using the equation $0.4 \times L \times W$ (L indicates length; W, width).[2] When tumor burdens reached ~100 mm^3 in volume, mice were randomized into 4 groups of 5 mice each to intraperitoneal injections of vehicle (10% polyethylene glycol, 3% Cremophor EL [Sigma-Aldrich], and 87% phosphate-buffered saline), MI-219 (100 mg/kg), dFdC (60 mg/kg), or both agents simultaneously at 50% of the single-agent dose (50 mg/kg MI-219; 30 mg/kg dFdC). Mice were killed by CO_2 asphyxiation when tumor size reached > 15 mm in any 1 direction according to institutional guidelines.

Table 1. Gene expression profiling of *wtp53* REC-1 MCL cells after exposure to MI-63

Gene	Fold change	GenBank accession no.	Description
Expression suppressed			
E2F8	−3.5	NM_024680	E2F transcription factor 8
RRM2	−3.3	BC001886	Ribonucleotide reductase M2 polypeptide
RRM2	−3.3	BE966236	Ribonucleotide reductase M2 polypeptide
CCNE2	−3.2	NM_004702	Cyclin E2
ESCO2	−2.9	AL120674	Establishment of cohesion 1 homolog (*Saccharomyces cerevisiae*)
RAD51AP1	−2.7	BE966146	RAD51-associated protein 1
TK1	−2.5	BC007986	Thymidine kinase 1 soluble
CDC6	−2.5	U77949	CDC6 cell division cycle 6 homolog (*S cerevisiae*)
MCM4	−2.4	AI859865	MCM4 minichromosome maintenance deficient 4 (*S cerevisiae*)
SPBC25	−2.3	AF225416	Spindle pole body component 25 homolog (*S cerevisiae*)
Expression induced			
BAX	+3	NM_004324	BCL2-associated X protein
SESN1	+3.2	NM_014454	Sestrin 1
WIG1	+3.7	NM_022470	p53 target zinc finger protein
FAS	+3.7	Z70519	FAS (TNF receptor superfamily, member 6)
PLK2	+3.8	NM_004110	Polo-like kinase 2 (*Drosophila*)
SULF2	+3.8	AL133001	Sulfatase 2
FAS	+4.3	AA164751	FAS (TNF receptor superfamily member 6)
FDXR	+4.7	NM_004110	Ferreddoxin reductase
CDKN1	+5.1	NM_000389	Cyclin-dependent kinase inhibitor 1A (p21, Cip1)
FAS	+6.5	NM_000043	FAS (TNF receptor superfamily member 6)

REC-1 cells were treated for 24 hours with vehicle or 5μM MI-63. Total cellular RNA was then extracted from triplicate experiments, and gene expression changes were detected using the Affymetrix Human Genome U133 Plus 2.0 array. Fold changes in genes were determined with vehicle- versus MI-63–treated cells using Ingenuity Pathway Analysis software. Ten representative up-regulated and down-regulated genes are shown from the profile.

Statistical analyses

Data were subjected to statistical analyses by calculation of the SEM. The significance of drug–effect relationships was further determined using 1-tailed unpaired *t* tests using Excel 2007 software (Microsoft). For the in vivo studies, an analysis of cooperative effects of MI-219 and dFdC on tumor growth data were performed using a Bayesian bootstrapping approach. We calculated $\Pr(\min(\mu_M,\mu_G) < \mu_C \text{ data})$, the posterior probability that the minimum of the 2 (posterior) means of the response, as evidenced by either final tumor volume, or average tumor growth rate, for MI-219 alone, μ_M, or dFdC alone, μ_G, was less than the (posterior) mean response for the combination, μ_C. This probability calculates the likelihood that average response in the combination arm will be less than the minimum of the 2 single agent arms. Cooperative effects are shown if this posterior probability is large. The statistical software R Version 2.120.0 (www.r-project.org) was used for all the analyses using 10 000 bootstrap samples.

Results

MI-63 induces down-regulation of RRM2 in MCL cells

We demonstrated previously that inhibition of HDM-2 by MI-63 was an effective strategy against MCL,[30] and sought to further explore the consequences of HDM-2 inhibition at the genomic level. Gene expression profiling of *wtp53* REC-1 cells exposed to MI-63 for 24 hours revealed enhanced expression of known p53 target genes (Table 1), such as *p21* and *Sestrin-1*. In addition, strong up-regulation of the apoptotic mediators tumor necrosis factor receptor superfamily, member 6 (Fas), and Bcl-2–associated X protein (Bax) was seen, consistent with stabilization of p53 by MI-63. This coincided with down-regulation of key genes involved in cell-cycle progression and cell proliferation, such as E2F transcription factor 8 (E2F8) and thymidine kinase. Of particular interest was the suppression of *RRM2*, which was reduced by more than 3-fold based on 2 different probes relative to the vehicle control. To further confirm this decrease, we measured RRM2 transcript levels by RT-PCR in Granta-519 and JVM-2, 2 other *wtp53* MCL cell lines. Compared with β_2M as a control, exposure of REC-1, Granta-519, or JVM-2 cells to either MI-63 or the *cis*-imidazoline HDM-2 inhibitor Nutlin resulted in decreased *RRM2* transcript levels in all cell lines (Figure 1A). Conversely, and as expected, HDM-2 inhibition increased transcript levels for RRM2B, which supplies excess dNTPs to cells undergoing genotoxic stress.[38] Suppression of transcription of RRM2 also resulted in a profound decrease in RRM2 expression at the protein level in Granta-519 and JVM-2 cells (Figure 1B) compared with β-actin as a control, and compared with RRM2B, which increased modestly after exposure to MI-63.

dFdC is synergistic with MI-63

We next considered the possibility that MI-63–mediated suppression of RRM2 could enhance sensitivity to dFdC, because RRM2 overexpression correlates with enhanced clinical dFdC resistance.[13] Exposure of MCL cell lines to MI-63 alone at 5μM for 24 hours resulted in the induction of cell death in 35% to 50% of *wtp53* cells (Figure 2A), whereas dFdC at 10nM produced apoptosis in 20% to 50% of cells. When both agents were added simultaneously for 24 hours, this increased the proportion of cells undergoing cell death to 90% in REC-1, 80% in Granta-519, and 60% in JVM-2 cells. Statistical analysis using an unpaired *t* test indicated that the combination of MI-63 and dFdC induced a significantly greater reduction in viability ($P < .05$) compared with either MI-63 or dFdC alone. The sole exception to this pattern were mutant (mut) p53 JeKo-1 cells, in which small amounts of cell death were seen because of their relative resistance to low doses of dFdC and complete lack of sensitivity to MI-63.

Combination chemotherapy regimens can have different efficacies depending on the sequence of addition of the drugs of interest. We therefore titrated MI-63 and dFdC against a panel of MCL cell lines and sought to determine what sequence of administration could be superior. We first determined the IC_{50} value of each cell

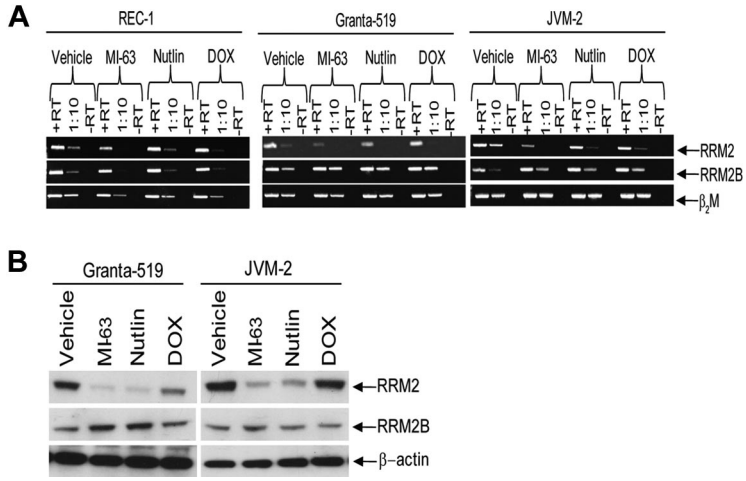

Figure 1. HDM-2 inhibitors decrease RRM2 polypeptide expression. (A) REC-1, Granta-519, and JVM-2 *wtp53* MCL cell lines were treated for 24 hours with either vehicle, 5μM MI-63, 5μM Nutlin, or 0.5μM doxorubicin (DOX) as a positive control for 24 hours. Qualitative PCR was performed to detect RRM2 and RRM2B mRNA levels, as well as β_2M as a loading control, and transcripts were visualized by native gel electrophoresis. Lanes marked +RT received 1 μL of cDNA stock solution, whereas those labeled with 1:10 received 1 μL of 1:10 dilution of +RT. Representative images are shown in both panels of 1 of 3 independent experiments. (B) Protein levels of RRM2 and RRM2B, as well as β-actin as a loading control, were determined in lysates from MCL cells treated as described in panel A.

line with both MI-63 and dFdC at 3 days (supplementa1 Figure 1A and B, respectively, available on the *Blood* Web site; see the Supplemental Materials link at the top of the online article). These calculated IC_{50} values allowed us to dose the agents in a 1:1 ratio based on the fold IC_{50} (0.25, 0.5, 1, 2, and 4×), as suggested for synergy calculations as set out in the methods of Chou and Talay.[36,37] Simultaneous administration of the 2 agents was compared with a schedule that allowed for pretreatment with 1 agent for 24 hours, followed by 48 hours with the second agent, for a total time of 72 hours. In Granta-519 cells, all 3 of these approaches resulted in enhanced cell killing compared with either agent alone at the lower drug concentrations (Figure 3B). CI analysis yielded CI values of 0.32 to 0.970, consistent with the presence of strong synergy for all 3 sequences (Table 2). Simultaneous addition of MI-63 and dFdC also showed synergy in REC-1 (CI, 0.33-0.93) and JVM-2 cells (0.71-0.81; Table 2). Pretreatment with MI-63 was synergistic in all 3 cell lines, particularly at low concentrations of 0.25× up to 1× of the IC_{50}, with CI values ranging as low as 0.28 in REC-1. However, synergy was lost at the higher concentrations tested of 2 and 4× the IC_{50}. In addition, pretreatment with dFdC demonstrated synergy in REC-1 cells (CI, 0.32-0.74), although this was lost at higher concentrations. In contrast, JVM-2 and Granta-519 cells showed synergy across the concentration range, with a CI range of 0.67 to 0.91 and 0.41 to 0.97, respectively.

Expression of RNR is regulated in a cell cycle–dependent manner,[39,40] and it was therefore of interest to analyze the impact of simultaneous addition of MI-63 and dFdC on *wtp53* MCL cells. Cell-cycle analysis indicated that MI-63 as a single agent induced a G_1 cell-cycle arrest (supplemental Figure 2), whereas dFdC induced a predominantly S-phase arrest. When both agents were combined, they generated a G_1 arrest in REC-1 and JVM-2 cells and a G_1/S arrest in Granta-519 cells. These findings suggest that MI-63 was able to override the S-phase arrest induced by dFdC and that the loss of RRM2 expression was because of a G_1 cell-cycle arrest, during which this subunit is known to be depleted due in part to its short half-life.[39] At the protein level, MI-63 as a single agent induced an accumulation of p53, p21, and HDM-2 in all 3 *wtp53* MCL cell lines compared with the vehicle control (Figure 2C). The same was true for the MI-63–dFdC combination, although the levels of these targets typically did not quite reach those seen with MI-63 alone. Enhanced levels of p21 would be expected to repress cyclin-dependent kinase 2, which would cause hypophosphorylation of Retinoblastoma protein and E2F, the latter of which is necessary for RRM2 transcription,[39,40] providing another mechanism for reduced RRM2 expression. Consistent with this mechanism, MI-63 alone decreased RRM2 levels in all 3 *wtp53* MCL cell lines (Figure 2C), whereas dFdC seemed to mildly induce RRM2, suggesting the involvement of an inducible chemoresistance pathway. When the 2 were combined, cells exposed to the MI-63–dFdC regimen showed reduced levels of RRM2 compared with dFdC alone, possibly accounting for the enhanced proapoptotic activity.

Synergy between MI-63 and dFdC is related to RRM2

HDM-2 inhibition triggers a p53-dependent death program, and because dFdC also activates apoptotic signaling in part through p53,[41] it was possible that the MI-63–dFdC combination was working through enhanced p53 induction. Western blotting of MCL cell lines treated with the combination did not reveal increased levels of p53, p21, or HDM-2 compared with either MI-63 or dFdC alone (Figure 2C), suggesting this was not the case. However, to test this more directly, we added an excess of dNTPs to the culture media of cells exposed to either agent or the combination, and then we evaluated the effects on cell death and signaling. Addition of dNTPs to MI-63–treated cells did not reduce cell death (Figure 3A), which was actually increased ($P = .003$), whereas dNTPs slightly attenuated the degree of cell death induced by dFdC alone ($P = .03$). When dNTPs were added to cells exposed to the combination, the synergistic effect was substantially blunted, with a reduction in cell death from 75% to 50% ($P < .01$), which was comparable with that induced by MI-63 alone (Figure 3A). This was associated with a decreased level of cleavage of PARP in the presence of dNTPs compared with that without supplemental nucleotides (Figure 3B). Notably, the levels of p53, p21, and HDM-2 that accumulated after exposure to the MI-63–dFdC combination were not dramatically changed by the presence of dNTPs, suggesting that p53 signaling was not affected. To further evaluate the role of suppression of RRM2 in the synergy of this combination, we generated REC-1 cells in which expression of this polypeptide was reduced by > 90% using a targeted shRNA (Figure 3C). Knockdown of RRM2 enhanced cell death to some extent because of both MI-63 and dFdC (Figure 3D), but the combination regimen was no longer able to show synergistic induction of apoptosis. These findings support the possibility that the MI-63–dFdC regimen is active through the ability of the HDM-2 inhibitor to reduce RRM2, thereby sensitizing to the ribonucleotide reductase inhibitor.

Activity of MI-63–dFdC against an MCL xenograft model

Because the combination of MI-63 and dFdC showed promising efficacy in vitro, we evaluated its activity against established MCL

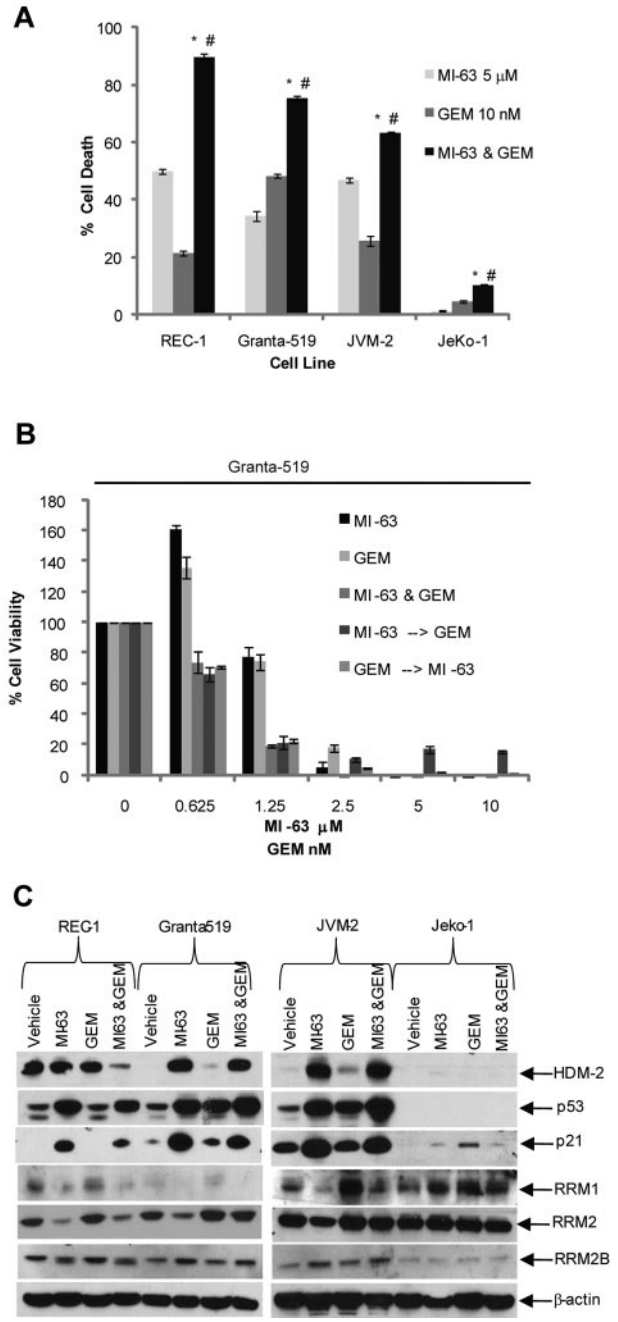

Figure 2. dFdC and MI-63 enhance cell death. (A) REC-1, Granta-519, and JVM-2, and the *mutp53* MCL cell line JeKo-1, were treated for 24 hours with vehicle, 5μM MI-63, 10nM dFdC (GEM), or both. Flow cytometric analysis was then performed after staining with annexin-V and TO-PRO-3, from which the proportion of cells undergoing apoptosis was calculated and normalized to the vehicle control group. Values represent the mean ± SE from 3 independent experiments. An unpaired *t* test was performed to evaluate for significance; $*P < .01$ relative to MI-63 alone; $\#P < .01$ relative to dFdC alone. (B) Granta-519 cells were incubated simultaneously with single agent MI-63 or dFdC for 72 hours. In parallel, cells were exposed either first to MI-63 for 24 hours followed by dFdC and MI-63 for 48 hours or to dFdC first for 24 hours followed later by MI-63 and dFdC for 48 hours. Cell viability was determined using the WST-1 reagent, and results are expressed as the percentage viability relative to the vehicle control, which was arbitrarily set at 100%. The presence of synergistic interactions was determined by calculation of the CI from the cell viabilities calculated across a serial dilution range of MI-63 or dFdC (Table 2). Each panel provides representative data from 1 of 3 independent experiments. (C) Protein levels of HDM-2, p53, RRM1, RRM2, RRM2B, and p21, and β-actin as a loading control, were determined by Western blotting of cellular lysates.

xenografts in an immunodeficient murine model using MI-219, the in vivo formulation of MI-63.[42] The latter agent alone, when given daily for 2 weeks at a dose of 100 mg/kg, slowed tumor growth ($P < .05$; Figure 4 top panel) to an average of 30 mm^3/day (Figure 4 bottom panel), compared with 74 mm^3/day for the vehicle control ($P = .002$). dFdC as a single agent, given at 60 mg/kg every 3 days for a total of only 2 weeks, also delayed tumor growth ($P < .05$; Figure 4 top panel), slowing it to 20 mm^3/day ($P = .09$; Figure 4 bottom panel). For the combination treatment, each agent was reduced in dose by 50%, and MI-219 at 50 mg/kg with dFdC at 30 mg/kg for 2 weeks slowed tumor growth to 5 mm^3/day ($P = .049$). Analysis of the cooperative effects between MI-219 and dFdC in terms of the final tumor volume indicated that the posterior probability of cooperative effect was found to be 0.9951, indicating that there was less than a 50 in 10 000 chance that the combination did not have a cooperative effect. For the average tumor growth rate, the cooperative effect was > 0.9977, demonstrating that there was less than a 25 in 10 000 chance that the combination did not have a cooperative effect, and a > 9975 in 10 000 chance that such an effect did exist. These analyses indicated a high level of evidence for the presence of cooperative effects of the combination treatment compared with the single agents. No toxicities were observed with either the single agents or the combination at the doses used in these cohorts.

MI-63 and dFdC are active against primary MCL cells

Regimens such as MI-63 and dFdC that show synergy preclinically may be attractive candidates for translation to the clinic; therefore, we evaluated the activity of this mechanism-based combination against patient-derived MCL cells. Nine primary samples were obtained, 6 of which harbored 2 *wtp53* alleles based on genomic DNA sequencing, whereas 2 were heterozygous, with 1 *wtp53* and 1 mutant p53 allele (supplemental Table 1). The majority of these samples were from patients with relapsed disease that had been previously treated with up to 4 prior lines of therapy (supplemental Table 1), whereas 2 were from patients with newly diagnosed disease. Exposure of these samples to MI-63 for 24 hours induced cell death in 20% to 80% of cells (Figure 5A). dFdC alone for 24 hours showed greater variability, in that although some samples were quite responsive, with cell death seen in up to 53%, such as the cells from patient 3, others were relatively resistant, with values as low as 3%, such as in patient 8. When the combination regimen was used for 24 hours, substantial enhanced effects consistent with synergy were seen in the samples from patients 1 to 4 ($P < .05$ relative to MI-63 alone or dFdC alone). Weakly additive effects were seen in patients 5, 7, and 9 ($P < .05$ relative to dFdC alone), whereas patients 6 and 8 showed no enhancement over what had been seen with MI-63 alone (Figure 5A).

To gain further insight into the sensitivity of these primary samples, we evaluated the expression levels of hENT-1; the dFdC transporter dCK, which activates and metabolizes dFdC; and RRM1 and RRM2 by quantitative real-time PCR. Primary samples 1 to 4 expressed both hENT-1 and dCK (Figure 5B), suggesting they could readily transport and metabolize dFdC and therefore respond well to the single-agent and combination therapy. Samples 5, 7, and 9, in contrast, had variable but generally lower expression levels of these genes (Figure 5B), possibly accounting for the lower level of enhanced cell death with the MI-63–dFdC regimen. Finally, samples 6 and 8, which showed no additive effects, also both expressed no hENT-1 (Figure 5B), although the former did show some sensitivity to single-agent dFdC (Figure 5A). All of the samples showed at least some expression of RRM1, but this expression was lower than that seen in some of the MCL cell lines (Figure 5B), and did not seem to correlate with sensitivity to dFdC.

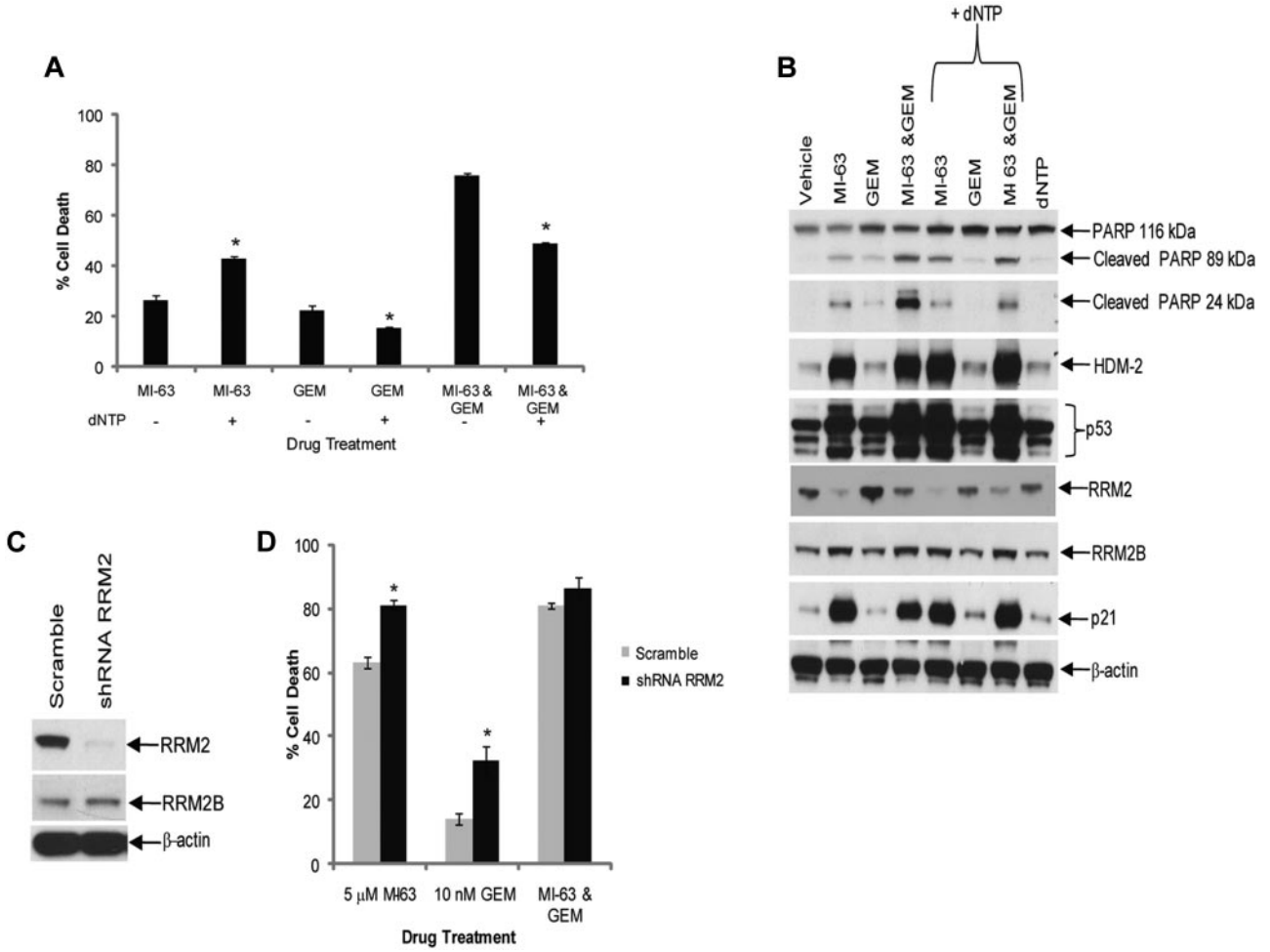

Figure 3. Excess dNTP reverses synergy between MI-63 and dFdC. (A) Granta-519 cells were incubated with vehicle, 5μM MI-63, 10nM dFdC (GEM), or both agents simultaneously for 24 hours, either without or with exogenous dNTPs at 50μM. Cell death was then determined by flow cytometry using annexin-V and TO-PRO-3 staining relative to the vehicle control. Each panel provides representative data from 1 of 3 independent experiments. An unpaired *t* test was performed comparing cells to which dNTPs had been added to those exposed to drug alone; $^*P < .05$. (B) Cellular lysates were probed for PARP, HDM-2, p53, RRM2, RRM2B, and p21, as well as β-actin as a loading control. (C) REC-1 cells were infected with Lentiviral particles carrying a scrambled sequence shRNA or an shRNA targeting RRM2, and stable cell lines were generated by drug selection. Cellular lysates were then probed for their content of RRM2, RRM2B, and β-actin as a loading control. (D) REC-1 shRNA cells were incubated with vehicle, 5μM MI-63, 10nM dFdC, or both agents simultaneously for 24 hours, and the proportion of cells undergoing apoptosis was determined by flow cytometry using annexin-V and TO-PRO-3. Statistically significant differences are defined as $^*P < .05$.

Similarly, RRM2 expression levels, which were more consistent between samples (Figure 5C), did not predict for sensitivity to either dFdC or MI-63–dFdC. However, in comparison with dCK, RRM1, and hENT-1 in the MCL cell lines, primary samples did express a relative abundance of RRM2 (Figure 5C). These findings support the translation of strategies to the clinic that suppress RRM2 levels in

Table 2. CI analysis of MCL cell lines treated with MI-63 and dFdC

	Fold × IC_{50} dFdC–MI-63				
	0.25	**0.50**	**1.0**	**2.0**	**4.0**
Simultaneous addition					
Granta-519	0.88*	0.88*	1.26	1.07	1.46
JVM-2	0.78*	0.73*	0.71*	0.81*	0.92
REC-1	0.33*	0.50*	0.93*	1.75	2.97
Pretreatment with MI-63, followed by dFdC					
Granta-519	0.32*	0.30*	0.49*	0.71*	1.13
JVM-2	0.98*	0.64*	0.40*	0.51*	0.15*
REC-1	0.28*	0.43*	0.78*	1.43	2.54
Pretreatment with dFdC, followed by MI-63					
Granta-519	0.41*	0.52*	0.91*	0.77*	0.97*
JVM-2	0.91*	0.70*	0.47*	0.12*	0.67*
REC-1	0.32*	0.54*	0.74*	1.38	2.46

The indicated *wtp53* MCL cell lines were incubated with MI-63 or dFdC alone, and their individual IC_{50} values were determined. Interactions were determined using a 1:1 ratio of MI-63 to dFdC by simultaneous addition of both drugs or in a sequence-specific manner for 72 hours, and CI values calculated using a range of IC_{50} values ranging from 0.25- to 4-fold the IC_{50} value of each drug in each cell line.

*Denotes a synergistic interaction.

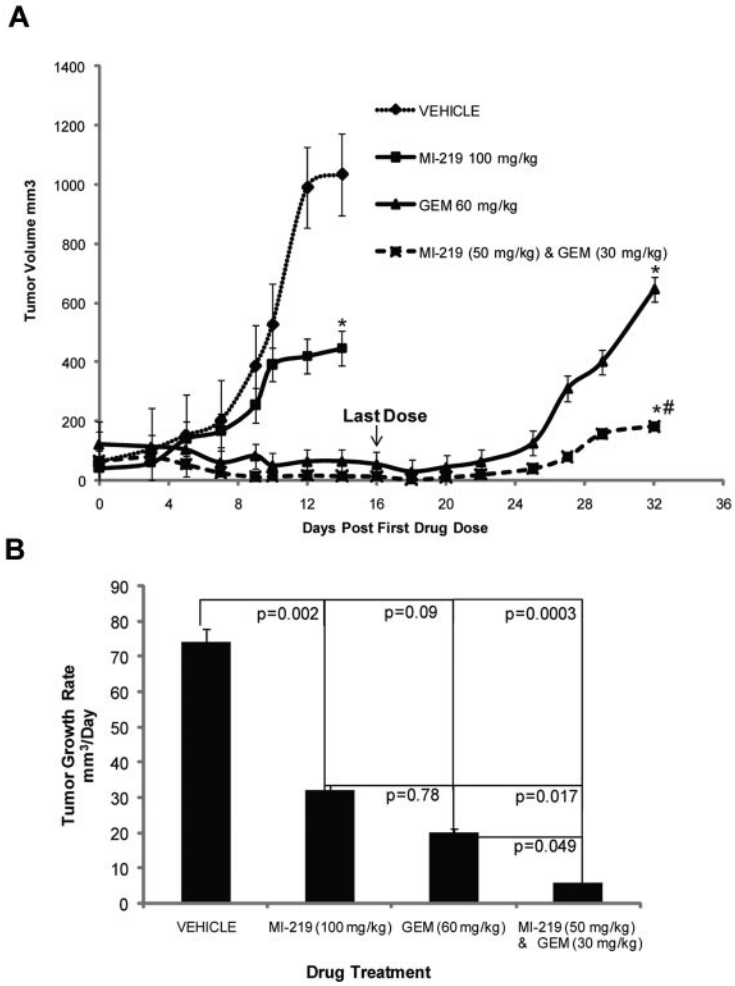

Figure 4. MI-63 and dFdC inhibit tumor growth in vivo. (A) Severe combined immunodeficiency mice were inoculated with Granta-519 cells subcutaneously and monitored until tumors were established. Five mice per group were then injected intraperitoneally with vehicle, MI-219 daily for 2 weeks, dFdC (GEM) every third day for 2 weeks, or both agents using the same schedules but at a 50% dose reduction. Tumor volumes were measured 3 times per week and are plotted as a function of time in the top panel. Statistically significant differences are defined as $*P < .05$ relative to the vehicle control and as $\#P < .05$ relative to MI-219 alone. In the bottom panel, the average tumor growth rate per day was calculated, and the *P* values of each group are shown relative to the vehicle group, as well as to MI-219 alone, or dFdC alone.

combination with dFdC, such as HDM-2 inhibition, for patients with relapsed mantle cell lymphoma that harbor wtp53 and express the human equilibrative nucleoside transporter and deoxycytidine kinase.

Discussion

MCL remains a challenging entity for the clinician, because there is as yet no widely accepted standard of care.[1-3] Immunochemotherapy strategies incorporating rituximab are commonly used in the front-line settings.[43,44] Younger patients may receive standard dose cyclophosphamide, doxorubicin, vincristine, and prednisone, followed by autologous stem cell transplantation, or more aggressive approaches with hyperfractionated cyclophosphamide regimens without transplantation.[43,44] These more intense approaches seem to increase complete response rates and overall survivals, but they cannot be applied in all cases given that the median age at the time of diagnosis is typically in the mid-1960s. In the latter patients, and even in a substantial proportion of those who can receive aggressive therapy, the disease is still not cured, and at the time of relapse is more aggressive, less chemosensitive, and has a poor postrelapse survival.[43,44] As a result, there is a strong imperative to develop new therapeutic agents and combinations and to also use them in a molecularly adapted manner, so that only those who would be most likely to benefit are exposed to the accompanying risks.

Our earlier preclinical studies had supported the possibility that HDM-2 inhibition was a rational strategy for therapy of MCL, and we therefore sought to develop combination regimens that could enhance this activity further. We first demonstrated that treatment of *wtp53* MCL models with MI-63 resulted in a profound decrease in expression of RRM2 (Table 1; Figure 1). This was associated with an arrest at G_1/S, and accumulation of p53 and its downstream target p21. RRM1, which is transcribed in S phase, has a long half-life of 20 hours, and remains at a constant level throughout the cell cycle.[45] In contrast, whereas RRM2 is also regulated in a cell cycle–dependent manner, and transcribed during S phase, it has a much shorter half-life of 3 hours,[46] and expression levels are therefore much more sensitive to interruption of its transcription and translation. The decrease in RRM2 with MI-63 indicated that the combination of MI-63 and dFdC could be synergistic, particularly because dFDCP is known to inhibit RRM2,[12] and in lung cancer patients decreased levels of RRM2 conveyed sensitivity to dFdC.[47] Consistent with this possibility, the combination of MI-63 and dFdC was effective against MCL, and reached the statistical criteria for synergistic interactions (Table 2). Furthermore, studies into the influence of the sequence dependence of dFdC and MI-63 demonstrated that simultaneous use of the 2 agents, as well as pretreatment with either one or the other, was effective (Figure 2). In addition, MI-63 seemed to overcome the S-phase arrest effect of dFdC, and the expected subsequent enhanced transcription of RRM2. A synergistic interaction was further supported by the MCL xenograft model, where a combination of MI-63 and dFdC showed

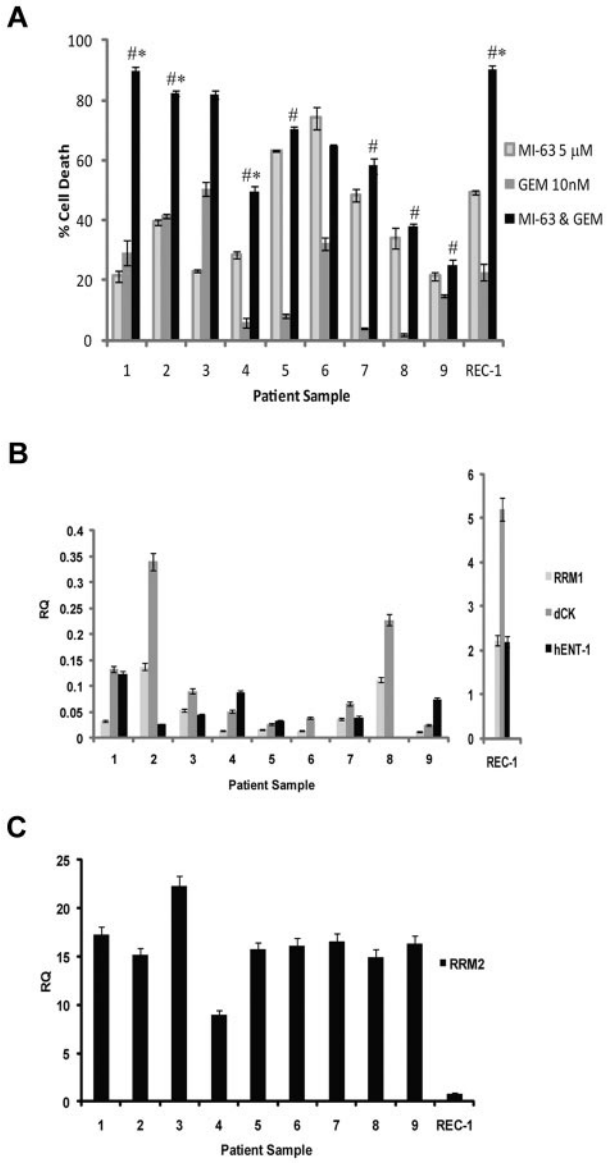

Figure 5. Synergistic activity of MI-63 and dFdC in MCL patient samples. (A) MCL cells were purified from the peripheral blood of patients with circulating neoplastic cells using magnetic-activated cell sorting and CD19 microbeads. These cells were then either exposed to 5μM MI-63, 10nM dFdC, or both agents simultaneously for 24 hours. Cell death was determined by flow cytometry using annexin-V and TO-PRO-3 staining relative to the vehicle-treated control, and REC-1 cells were included as an additional control. Each panel provides representative data from 1 of 3 independent experiments, and $*P < .05$ denote significance relative to MI-63 alone, and $\#P < .05$ denote significance relative to dFdC alone. (B) Aliquots of each of the primary samples analyzed in panel A also were subjected to RNA extraction, cDNA was synthesized, and the levels of *RRM1*, *dCk*, *hENT-1*, and *RRM2* were measured by quantitative real-time PCR using the ΔΔCT method with the JVM-2 cell line used as a relative calibrator. The transcript level in REC-1 cells also was measured as a control and is plotted on a separate scale because of their high expression of *RRM1*, *dCK*, and *hENT-1*. (C) Real-time PCR analysis of RRM2 transcript levels in MCL patient samples is shown, along with REC-1 as a cell line control.

enhanced tumor growth delay, even at a 50% dose reduction compared with either of the single agents (Figure 4).

Treatment of primary samples ex vivo also yielded promising results despite that 6 of the 9 patients had received prior dose-intensive chemotherapy in the form of either stem cell transplantation or hyperfractionated cyclophosphamide (supplemental Table 1). Notably, the efficacy against patient samples also showed some dependency on the expression of the nucleoside transporter hENT-1 and on dCK (Figure 5). Of particular interest was that the levels of hENT-1, dCK, and RRM1 were substantially higher in the MCL cell line REC-1 and lower in the MCL patient samples. Conversely, RRM2 levels were substantially higher in the primary lymphoma cells than in the REC-1 model, and both of these would be expected to negatively impact on the sensitivity of MCL in vivo to dFdC. Indeed, the expression of hENT-1 has been shown to be a mediator of sensitivity to dFdC in MCL, and a good correlation was found between hENT-1 expression and uptake and sensitivity to this nucleoside analog in previous studies.[39] Similarly, RRM2 overexpression has been reported as a mechanism of resistance to dFdC in cell lines,[13] and overexpression was correlated with poor survival in lung adenocarcinoma patients treated with docetaxel and dFdC.[47] We observed a synergistic effect between MI-63 and dFdC in some of the MCL patient samples, whereas others were resistant to this combination. The resistance may be linked to other cellular factors beyond those we evaluated here, because dFdC can be transported, metabolized, and inactivated by additional factors, including the human equilibrative nucleoside transporter-2, the human concentrative nucleoside transporters-1 and -2, cytidine deaminase, and 5′-nucleotidase, among others. For example, 1 MCL patient who was resistant to nucleoside analogs demonstrated abundant hENT-1, dCK, and minimal 5′-nucleotidases, but it was still resistant on presentation to fludarabine and dFdC.[48] Moreover, alterations in genes such as ataxia telangiectasia mutated and p53 may influence resistance to nucleoside analogues,[49] particularly in MCL given the high rate of changes in DNA damage pathways.[21,22] It is also likely that the prior chemotherapy regimens patients received will have had an effect on the sensitivity to the MI-63–dFdC combination, particularly in those who received regimens incorporating DNA-damaging agents.

The *cis*-imidazoline HDM-2 inhibitor RO5045337 is currently undergoing phase 1 trials targeting patients both with solid tumors (NCT00559533) and with hematologic malignancies such as chronic lymphocytic leukemia (NCT00623870). With regard to the latter study, a recent preliminary report indicated that 47 patients had been treated to date, and pharmacodynamic studies had shown induction of p53 target genes such as p21, Bax, and Fas.[50] Dose escalation was continuing upward in 2 strata from 810 and 1920 mg/m^2/day, respectively, and clinical activity was seen in 1 patient with acute myeloid leukemia at 360 mg/m^2 who had achieved an ongoing complete remission for > 9 months. These preliminary results of the first clinical trial of an HDM-2 inhibitor provide a proof of principle that the p53–HDM-2 axis can be manipulated with specific inhibitors not only preclinically but also clinically. In combination with our current data, which provide a molecular rationale for combining an HDM-2 inhibitor and dFdC in models of MCL, especially if they have wt p53 and express hENT-1 and dCK, these findings provide a strong framework for translation of this approach to the clinic. Moreover, because nucleoside analogs are used in other subtypes of non-Hodgkin lymphomas, as well as other hematologic malignancies, including acute and chronic leukemias, both in the relapsed and in some front-line settings, investigation of this regimen may be warranted preclinically and clinically in those settings as well.

Acknowledgments

Primary tumor samples were provided by the M. D. Anderson Cancer Center Lymphoma Tissue Bank (P50 CA136411). Flow cytometry services were provided by the M. D. Anderson Flow Cytometry Core Facility, and p53 gene sequencing was performed by the DNA Analysis Core Facility, all of which are supported by Cancer Center Support grant CA 16672. The authors are grateful to Shaomeng

Wang (University of Michigan) for providing MI-63 and MI-219 and to Lance Leopold (Ascenta Therapeutics) for valuable suggestions.

R.J.J., a Lymphoma Research Foundation Fellow, acknowledges support from the Lymphoma Research Foundation. R.Z.O., a Leukemia & Lymphoma Society Scholar in Clinical Research, acknowledges support from the National Cancer Institute (grant P50 CA142509).

Authorship

Contribution: R.J.J. designed and performed all of the research and animal experiments and wrote the manuscript; L.E.F., J.E.R., and M.W. obtained patient consent and samples; R.S. and S.N. were essential for helping with processing of patient samples and maintaining the lymphoma tissue bank; D.Y. provided the MI-63 and MI-219 and method; V.B. performed statistical support and analysis; and R.Z.O. supervised all the research completed here and offered valuable suggestions and manuscript editing.

Conflict-of-interest disclosure: D.Y. is an employee of and stockholder in Ascenta Therapeutics. The remaining authors declare no competing financial interests.

Correspondence: Richard J. Jones, Department of Lymphoma and Myeloma, The University of Texas M. D. Anderson Cancer Center, 7455 Fannin St, Unit 403, Houston, TX 77054; e-mail: rjones@mdanderson.org.

References

1. Campo E, Raffeld M, Jaffe ES. Mantle-cell lymphoma. *Semin Hematol.* 1999;36(2):115-127.
2. Martin P, Leonard JP. Novel therapeutic targets in mantle cell lymphoma. *Expert Opin Ther Targets.* 2007;11(7):929-940.
3. O'Connor OA. Mantle cell lymphoma: identifying novel molecular targets in growth and survival pathways. *Hematology Am Soc Hematol Educ Program.* 2007;2007:270-276.
4. Orlowski RZ, Stinchcombe TE, Mitchell BS, et al. Phase I trial of the proteasome inhibitor PS-341 in patients with refractory hematologic malignancies. *J Clin Oncol.* 2002;20(22):4420-4427.
5. O'Connor OA, Wright J, Moskowitz C, et al. Phase II clinical experience with the novel proteasome inhibitor bortezomib in patients with indolent non-Hodgkin's lymphoma and mantle cell lymphoma. *J Clin Oncol.* 2005;23(4):676-684.
6. Goy A, Younes A, McLaughlin P, et al. Phase II study of proteasome inhibitor bortezomib in relapsed or refractory B-cell non-Hodgkin's lymphoma. *J Clin Oncol.* 2005;23(4):667-675.
7. Fisher RI, Bernstein SH, Kahl BS, et al. Multicenter phase II study of bortezomib in patients with relapsed or refractory mantle cell lymphoma. *J Clin Oncol.* 2006;24(30):4867-4874.
8. Witzig TE, Geyer SM, Ghobrial I, et al. Phase II trial of single-agent temsirolimus (CCI-779) for relapsed mantle cell lymphoma. *J Clin Oncol.* 2005;23(23):5347-5356.
9. Witzig TE, Reeder CB, Laplant BR, et al. A phase II trial of the oral mTOR inhibitor everolimus in relapsed aggressive lymphoma. *Leukemia.* 2011; 25(2):341-347.
10. Wiernik PH, Lossos IS, Tuscano JM, et al. Lenalidomide monotherapy in relapsed or refractory aggressive non-Hodgkin's lymphoma. *J Clin Oncol.* 2008;26(30):4952-4957.
11. Habermann TM, Lossos IS, Justice G, et al. Lenalidomide oral monotherapy produces a high response rate in patients with relapsed or refractory mantle cell lymphoma. *Br J Haematol.* 2009; 145(3):344-349.
12. Dumontet C, Morschhauser F, Solal-Celigny P, et al. Gemcitabine as a single agent in the treatment of relapsed or refractory low-grade non-Hodgkin's lymphoma. *Br J Haematol.* 2001;113(3):772-778.
13. Hitz F, Martinelli G, Zucca E, et al. A multicentre phase II trial of gemcitabine for the treatment of patients with newly diagnosed, relapsed or chemotherapy resistant mantle cell lymphoma: SAKK 36/03. *Hematol Oncol.* 2009;27(3):154-159.
14. Chau I, Watkins D, Cunningham D. Gemcitabine and its combinations in the treatment of malignant lymphoma. *Clin Lymphoma.* 2002;3(2):97-104.
15. Heinemann V, Schulz L, Issels RD, Plunkett W. Gemcitabine: a modulator of intracellular nucleotide and deoxynucleotide metabolism. *Semin Oncol.* 1995;22(4 suppl 11):11-18.
16. Huang P, Chubb S, Hertel LW, Grindey GB, Plunkett W. Action of 2′,2′-difluorodeoxycytidine on DNA synthesis. *Cancer Res.* 1991;51(22):6110-6117.
17. Heinemann V, Xu YZ, Chubb S, et al. Inhibition of ribonucleotide reduction in CCRF-CEM cells by 2′,2′-difluorodeoxycytidine. *Mol Pharmacol.* 1990;38(4):567-572.
18. Baker CH, Banzon J, Bollinger JM, et al. 2′-Deoxy-2′-methylenecytidine and 2′-deoxy-2′,2′-difluorocytidine 5′-diphosphates: potent mechanism-based inhibitors of ribonucleotide reductase. *J Med Chem.* 1991;34(6):1879-1884.
19. Goan YG, Zhou B, Hu E, Mi S, Yen Y. Overexpression of ribonucleotide reductase as a mechanism of resistance to 2,2-difluorodeoxycytidine in the human KB cancer cell line. *Cancer Res.* 1999;59(17):4204-4207.
20. Shao J, Zhou B, Chu B, Yen Y. Ribonucleotide reductase inhibitors and future drug design. *Curr Cancer Drug Targets.* 2006;6(5):409-431.
21. Jares P, Campo E. Advances in the understanding of mantle cell lymphoma. *Br J Haematol.* 2008;142(2):149-165.
22. Dreyling M, Hoster E, Bea S, et al. Update on the molecular pathogenesis and clinical treatment of Mantle Cell Lymphoma (MCL): minutes of the 9th European MCL Network conference. *Leuk Lymphoma.* 2010;51(9):1612-1622.
23. Haidar JH, Neiman RS, Orazi A, Albitar M, McCarthy LJ, Heerema N. mdm-2 oncoprotein expression associated with deletion of the long arm of chromosome 12 in a case of mantle cell lymphoma with blastoid transformation [corrected]. *Mod Pathol.* 1996;9(4):355-359.
24. Møller MB, Nielsen O, Pedersen NT. Oncoprotein MDM2 overexpression is associated with poor prognosis in distinct non-Hodgkin's lymphoma entities. *Mod Pathol.* 1999;12(11):1010-1016.
25. Solenthaler M, Matutes E, Brito-Babapulle V, Morilla R, Catovsky D. p53 and mdm2 in mantle cell lymphoma in leukemic phase. *Haematologica.* 2002;87(11):1141-1150.
26. Hernández L, Bea S, Pinyol M, et al. CDK4 and MDM2 gene alterations mainly occur in highly proliferative and aggressive mantle cell lymphomas with wild-type INK4a/ARF locus. *Cancer Res.* 2005;65(6):2199-2206.
27. Greiner TC, Dasgupta C, Ho VV, et al. Mutation and genomic deletion status of ataxia telangiectasia mutated (ATM) and p53 confer specific gene expression profiles in mantle cell lymphoma. *Proc Natl Acad Sci U S A.* 2006;103(7):2352-2357.
28. Hartmann E, Fernandez V, Stoecklein H, Hernandez L, Campo E, Rosenwald A. Increased MDM2 expression is associated with inferior survival in mantle-cell lymphoma, but not related to the MDM2 SNP309. *Haematologica.* 2007;92(4): 574-575.
29. Harris SL, Levine AJ. The p53 pathway: positive and negative feedback loops. *Oncogene.* 2005; 24(17):2899-2908.
30. Jones RJ, Chen Q, Voorhees PM, et al. Inhibition of the p53 E3 ligase HDM-2 induces apoptosis and DNA damage-independent p53 phosphorylation in mantle cell lymphoma. *Clin Cancer Res.* 2008;14(17):5416-5425.
31. Tabe Y, Sebasigari D, Jin L, et al. MDM2 antagonist nutlin-3 displays antiproliferative and proapoptotic activity in mantle cell lymphoma. *Clin Cancer Res.* 2009;15(3):933-942.
32. Drakos E, Atsaves V, Li J, et al. Stabilization and activation of p53 downregulates mTOR signaling through AMPK in mantle cell lymphoma. *Leukemia.* 2009;23(4):784-790.
33. Jin L, Tabe Y, Kojima K, et al. MDM2 antagonist Nutlin-3 enhances bortezomib-mediated mitochondrial apoptosis in TP53-mutated mantle cell lymphoma. *Cancer Lett.* 2010;299(2):161-170.
34. Jones RJ, Dickerson S, Bhende PM, Delecluse HJ, Kenney SC. Epstein-Barr virus lytic infection induces retinoic acid-responsive genes through induction of a retinol-metabolizing enzyme, *DHRS9. J Biol Chem.* 2007;282(11):8317-8324.
35. Kuhn DJ, Chen Q, Voorhees PM, et al. Potent activity of carfilzomib, a novel, irreversible inhibitor of the ubiquitin-proteasome pathway, against preclinical models of multiple myeloma. *Blood.* 2007;110(9):3281-3290.
36. Chou TC. The median-effect principle and the combination index for quantitation of synergism and antagonism. In: Chou TC, Rideout DC, eds. Synergism and antagonism in chemotherapy. San Diego, CA: Academic Press; 1991:61-102.
37. Chou TC, Talalay P. Quantitative analysis of dose-effect relationships: the combined effects of multiple drugs or enzyme inhibitors. *Adv Enzyme Regul.* 1984;22:27-55.
38. Tanaka H, Arakawa H, Yamaguchi T, et al. A ribonucleotide reductase gene involved in a p53-dependent cell-cycle checkpoint for DNA damage. *Nature.* 2000;404(6773):42-49.
39. Engström Y, Eriksson S, Jildevik I, Skog S, Thelander L, Tribukait B. Cell cycle-dependent expression of mammalian ribonucleotide reductase. Differential regulation of the two subunits. *J Biol Chem.* 1985;260(16):9114-9116.
40. Björklund S, Skog S, Tribukait B, Thelander L. S-phase-specific expression of mammalian ribonucleotide reductase R1 and R2 subunit mRNAs. *Biochemistry.* 1990;29(23):5452-5458.
41. Achanta G, Pelicano H, Feng L, Plunkett W, Huang P. Interaction of p53 and DNA-PK in response to nucleoside analogues: potential role as a sensor complex for DNA damage. *Cancer Res.* 2001;61(24):8723-8729.
42. Shangary S, Qin D, McEachern D, et al. Temporal activation of p53 by a specific MDM2 inhibitor is selectively toxic to tumors and leads to complete tumor growth inhibition. *Proc Natl Acad Sci U S A.* 2008;105(10):3933-3938.

43. Williams ME, Dreyling M, Winter J, Muneer S, Leonard JP. Management of mantle cell lymphoma: key challenges and next steps. *Clin Lymphoma Myeloma Leuk.* 2010;10(5):336-346.

44. Goy A, Kahl B. Mantle cell lymphoma: the promise of new treatment options [published online ahead of print December 16, 2010]. *Crit Rev Oncol Hematol.* doi:10.1016/j.critrevonc.2010.09.003.

45. Mann GJ, Musgrove EA, Fox RM, Thelander L. Ribonucleotide reductase M1 subunit in cellular proliferation, quiescence, and differentiation. *Cancer Res.* 1988;48(18):5151-5156.

46. Eriksson S, Graslund A, Skog S, Thelander L, Tribukait B. Cell cycle-dependent regulation of mammalian ribonucleotide reductase. The S phase-correlated increase in subunit M2 is regulated by de novo protein synthesis. *J Biol Chem.* 1984;259(19):11695-11700.

47. Souglakos J, Boukovinas I, Taron M, et al. Ribonucleotide reductase subunits M1 and M2 mRNA expression levels and clinical outcome of lung adenocarcinoma patients treated with docetaxel/gemcitabine. *Br J Cancer.* 2008;98(10):1710-1715.

48. Reiman T, Graham KA, Wong J, et al. Mechanisms of resistance to nucleoside analogue chemotherapy in mantle cell lymphoma: a molecular case study. *Leukemia.* 2002;16(9):1886-1887.

49. Ferrer A, Marce S, Bellosillo B, et al. Activation of mitochondrial apoptotic pathway in mantle cell lymphoma: high sensitivity to mitoxantrone in cases with functional DNA-damage response genes. *Oncogene.* 2004;23(55):8941-8949.

50. Andreeff M, Kojima K, Padmanabhan S, et al. A multicenter, open-label, phase I study of single Agent RG7112, a first in class p53-MDM2 antagonist, in patients with relapsed/refractory acute myeloid and lymphoid leukemias (AML/ALL) and refractory chronic lymphocytic leukemia/small cell lymphocytic lymphomas (CLL/SCLL) [abstract]. *Blood.* 2010;116:Abstract 657.